

Entanglement and spectra in topological many-body localized phases

K. S. C. Decker,¹ D. M. Kennes,¹ J. Eisert,¹ and C. Karrasch²

¹*Dahlem Center for Complex Quantum Systems and Fachbereich Physik, Freie Universität Berlin, 14195 Berlin, Germany and*

²*Technische Universität Braunschweig, Institut für Mathematische Physik, Mendelssohnstrae 3, 38106 Braunschweig, Germany*

Many-body localized systems in which interactions and disorder come together defy the expectations of quantum statistical mechanics: In contrast to ergodic systems, they do not thermalize when undergoing non-equilibrium dynamics. What is less clear, however, is how topological features interplay with many-body localized phases as well as the nature of the transition between a topological and a trivial state within the latter. In this work, we numerically address these questions, using a combination of extensive tensor network calculations, specifically DMRG-X, as well as exact diagonalization, leading to a comprehensive characterization of Hamiltonian spectra and eigenstate entanglement properties. We advocate that the scaling properties of entanglement features characterize many-body localized systems both in topological and trivial situations, but that no longer the entanglement entropy, but mixed-state entanglement measures such as the negativity — a concept inherited from quantum information — can meaningfully be made use of, due to the close to degenerate energy levels.

The paradigm of *many-body localization* (MBL) uplifts Anderson localization to a regime in which genuine interactions matter.^{1,2} It manifestly breaks ergodicity and expectations from quantum statistical mechanics³: once pushed out of equilibrium,^{4–6} such quantum many-body systems will equilibrate, but retain too much memory of the initial conditions to fully thermalize. Indeed, the phenomenon of many-body localization is multi-faceted, giving rise to a plethora of phenomena that seem to have little in common at first sight. It is accompanied by an extensive number of quasi-local constants of motion,⁷ by eigenstates in the bulk that generically exhibit *entanglement area laws*,^{8,9} and by a peculiar logarithmic growth of entanglement entropies.^{10,11} Reflecting this rich phenomenology, it is no surprise that the transition between an ergodic and localized regime has moved into the focus of attention.^{12–16}

What is less clear, at the same time, is how types of order come to play in this state of affairs. It has been shown that excited eigenstates can exhibit signatures of topological order,^{17–19} yet the precise mechanism let alone the transition to the ergodic regime are not fully understood. This is partially due to a lack of methods to address this question. Tensor network methods^{20–22} have been extended to be able to address properties of highly excited states^{23–25}, prominently the *DMRG-X* method,²⁶ generalizing the *density matrix renormalization group* (DMRG) method²⁷ to capture highly excited states that feature an entanglement area-law.

In contrast, addressing the question how MBL and topological properties compete or co-exist has only recently moved into the center of attention. Naively, one would expect topological order to be absent in a regime in which disorder dominates driving the system into a MBL state. However, recently a model was proposed exemplifying that this is not always the case.^{18,19} We elaborate on this question using a combination of exact diagonalization and extensive *tensor network*, specifically DMRG-X, approaches to determine the topological properties in the presence of MBL. By studying typical hallmarks of MBL physics as well as topology, such as the energy level statics, fluctuations of local observables and entropy, we determine the phase diagram of the model proposed in Refs.^{19,28}, with variants discussed in Refs.^{18,29}. We do so in dependence of its genuine interaction parameters, see Fig. 1.

A key observation of this work is that in order to achieve this goal, we need to replace the concept of entanglement entropy by *mixed-state entanglement measures*. This is due to the fact that in the presence of topological order, edge excitations lead to the appearance of almost degenerate quadruples of excited states which share the same local properties in the bulk of the system (so almost everywhere). As a consequence, the DMRG-X procedure, which relies on the fact that eigenstates close in energy differ substantially in real space (which holds true in the non-topological MBL regime), fails to resolve single eigenstates and instead determines a linear combination of these quadruples' quantum states in the topological phase. Observables characterized by the bulk-behavior, which are (almost) independent of the choice of this linear combination, can be determined reliably, while we will show that entanglement scaling is artificially reduced using DMRG-X.

Model. To be concrete, we focus on a specific model Hamiltonian, yet one that clearly shows the signatures at the heart of our argument. The system is governed by^{19,28}

$$H = \sum_i (\lambda_i \sigma_{i-1}^z \sigma_i^x \sigma_{i+1}^z + h_i \sigma_i^x + V_i \sigma_i^x \sigma_{i+1}^x), \quad (1)$$

where $\sigma_i^{x,y,z}$ denote Pauli matrices supported on site i . Unless mentioned otherwise, we will work with a system of size L and open boundary conditions. The real pre-factors λ_i , h_i , and V_i are random variables drawn from a Gaussian distribution with a standard deviation of $\sigma_{\lambda,h,V}$. We choose $\sigma_\lambda = 1$ for the rest of this work. Note that for $V_i = 0$, the system can be mapped to non-interacting fermions via a Jordan-Wigner transformation.

Simple limits. For $h_i = V_i = 0$, the Hamiltonian of Eq. (1) takes the form of a sum of mutually-commuting operators, $H_0 = \sum_i \lambda_i O_i$ with $O_i = \sigma_{i-1}^z \sigma_i^x \sigma_{i+1}^z$ and $[O_i, O_j] = 0$.¹⁹ It can thus be treated analytically. A system with open boundaries features free spin-1/2 edge excitations generated by the Pauli operators $\Sigma_L^x = \sigma_1^x \sigma_2^z$, $\Sigma_L^y = \sigma_1^y \sigma_2^z$, $\Sigma_L^z = \sigma_1^z$ (and similarly at the right end of the chain), which commute with H_0 . Each eigenvalue of H_0 is thus four-fold degenerate, and the system is in a topological phase at arbitrary energies.

One can show that each eigenstate of H_0 can be expressed as a *matrix-product state* (MPS) with a bond dimension of

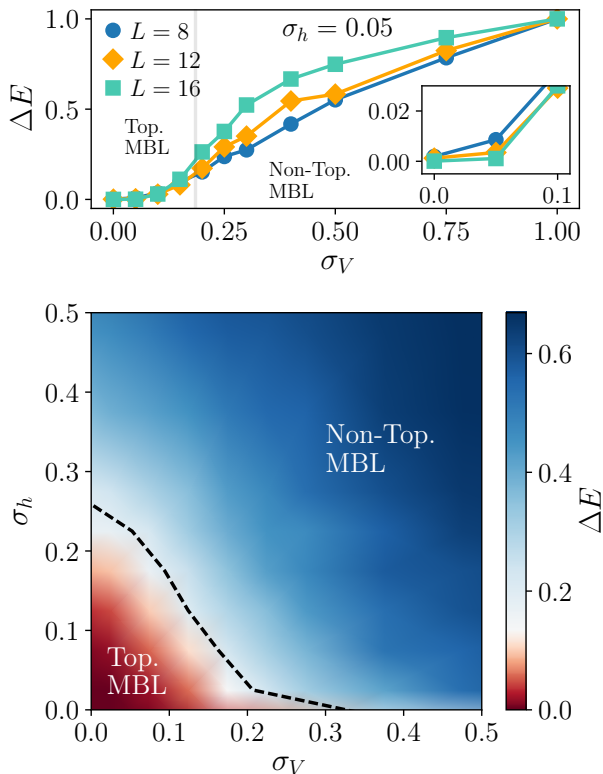


FIG. 1. *Top panel:* Normalized distance ΔE between the highest and lowest energies of four consecutive mid-spectrum (high-energy) eigenstates as a function of σ_V for fixed $\sigma_h = 0.05$ and various system sizes. The window from which the eigenstates are taken ranges from 0.4 to 0.6 in terms of the reduced energy ϵ with ΔE being normalized against its maximum at $\sigma_h = 0.05$ and $\sigma_V = 1.0$. The topological phase has a four-fold degenerate spectrum (associated with the edge excitations) and is characterized by $\Delta E \rightarrow 0$ in the thermodynamic limit. The eigenstates are non-degenerate in the trivial phase ($\Delta E > 0$). Each data point represents an average over at least 99 disorder realizations. *Bottom panel:* High-energy (mid-spectrum) phase diagram in the $\sigma_h - \sigma_V$ plane for $L = 14$. This time, ΔE is normalized against $\sigma_h = 1.0$ and $\sigma_V = 1.0$. The crossover between the topological and trivial phase (dashed line) is defined as $\Delta E = 0.2$. The system remains many-body localized for any of these parameters (see Fig. 2). Here, each data point was evaluated with at least 99 disorder realizations as well.

$\chi = 2$ and hence features an *entanglement area law*,³⁰ which can be seen as a signature of *localization*. To this end, we rewrite $H_0 = e^{ih} \tilde{H}_0 e^{-ih^\dagger}$ with $h = \sum_i \sigma_i^x \sigma_{i+1}^x$ and $\tilde{H}_0 = \sum_i \lambda_i \sigma_i^z$. The eigenstates of \tilde{H}_0 are product states. The operator e^{ih} simply acts as a product of mutually commuting two-site quantum gates and transforms each product eigenstate into *matrix product states* with a bond dimension of two upon conjugation: For every product state vector $|P\rangle$, $e^{ih}|P\rangle$ is such a matrix product state vector.

In the converse limit where h_i and V_i are large, the Hamiltonian takes the form of a classical Ising model whose eigenstates are product states in the σ^x -basis; they are thus trivially localized but do not feature topological properties. This sug-

gests that the system may be localized for any values of $\sigma_{h,V}$ but that a transition between a topological MBL phase and a trivial MBL phase occurs when $\sigma_{h,V}$ are increased. We will now confirm this scenario explicitly using a combination of exact diagonalization and DMRG-X numerics, when applicable (see above).

Topology: Spectrum degeneracy. We now show that the topological properties of highly-excited states survive for $h_i \neq 0$, $V_i \neq 0$. To this end, Eq. (1) is first solved by exact diagonalization. We characterize the topological phase by a four-fold degeneracy of the spectrum in the thermodynamic limit (finite systems feature exponential corrections) and the trivial phase by a non-degenerate spectrum.

In the top panel of Fig. 1, we plot the normalized distance between the four consecutive eigenvalues ΔE , which serves as a measure for the degeneracy of the spectrum, as a function of σ_V for fixed $\sigma_h = 0.05$ and various system sizes L . Here, ΔE is normalized against its maximum (at $\sigma_h = 0.05$ and $\sigma_V = 1.0$), with the phase boundary being defined at $\Delta E = 0.2$ in this normalization. The disorder sampling has been carried out such that the error is smaller than the symbol size, and we limited ourselves to mid-spectrum (high-energy) states in a window $[0.4, 0.6]$ in terms of the reduced energy $\epsilon = (E - E_{\min}) / (E_{\max} - E_{\min})$, with E_{\min} and E_{\max} the minimum and maximum energy of the spectrum, respectively. For small (large) σ_V , ΔE decreases (increases) with L . The data of Fig. 1 thus indicates that a transition between a high-energy topological phase and a trivial phase occurs around $\sigma_V \sim 0.2$. In the bottom panel of Fig. 1, we show the degeneracy ΔE for fixed $L = 14$ in the $\sigma_h - \sigma_V$ plane. The phase boundary (dashed line) was defined via $\Delta E = 0.2$, with ΔE again being normalized against its maximum (which occurs at ΔE at $\sigma_V = 1.0$ and $\sigma_h = 1.0$).

Many-body localization: Adjacent gap ratio. As a next step, we provide strong evidence that the system remains localized for arbitrary values of σ_h and σ_V . In the top panels of Fig. 2, we show the distribution of the adjacent gap ratio (AGR) r for the mid-spectrum states $\epsilon \in [0.4, 0.6]$ and at least 99 repetitions of disorder configurations for fixed $\sigma_h = 0.05$, various $\sigma_V = 0.1, 0.5, 1.0$, and $L = 14$. For $\sigma_V = 0.1$, the system is in the topological phase and thus features a sharp peak at $r = 0$, which signals the extensive number of quadruples of (close to degenerate) eigenstates given by the edge excitations. This peak vanishes when σ_V is increased. The tail of the distribution always takes a Poissonian form, which is a hallmark of localization. For periodic boundary conditions, the spectrum is always non-degenerate, and the peak around $r = 0$ is absent from the AGR (as it is rooted in the edge excitations). The AGR is of a Poissonian form for arbitrary σ_V (data not shown, but note the bottom panel of Fig. 2).

In the bottom panel of Fig. 2, we show the relative weight of the Poissonian tail as a function of σ_V for fixed $\sigma_h = 0.05$. For small (large) σ_V , this weight decreases (increases) with the system size, implying that more (less) weight is shifted into the peak at $r = 0$. This again provides strong substance that a transition between a topological and a trivial phase takes place around $\sigma_V \sim 0.2$. For periodic boundary conditions, the peak is absent and the AGR is of a Poissonian form.

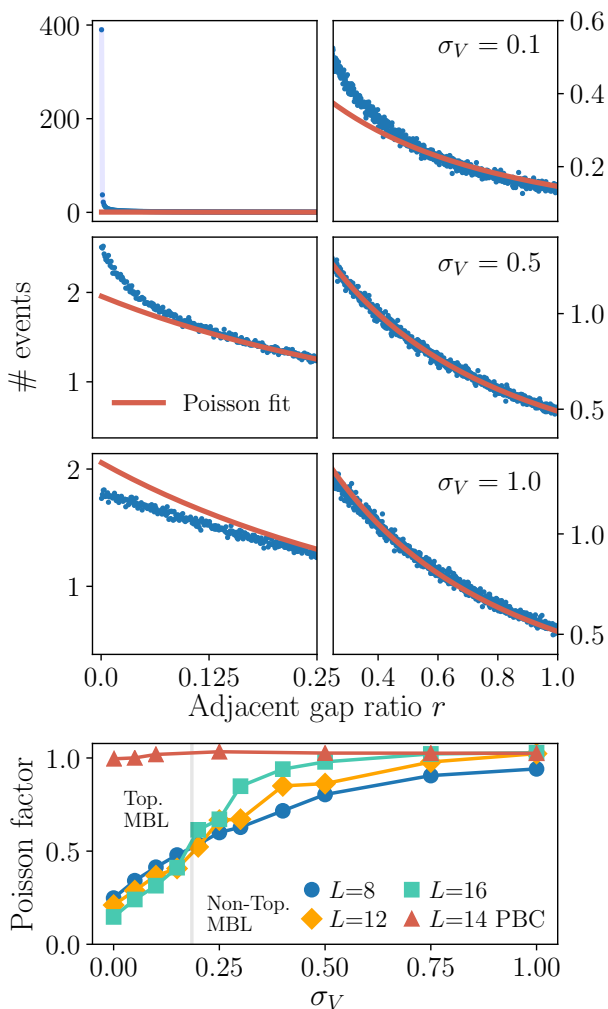


FIG. 2. *Top panel:* Distribution of the adjacent gap ratio in mid-spectrum eigenstates for fixed $\sigma_h = 0.05$, various σ_V , and $L = 14$. The eigenstates are all from the interval $[0.4, 0.6]$ in terms of the reduced energy ϵ and the distributions were drawn from at least 99 disorder realizations. The sharp peak at $r = 0$ is a signal of the degenerate spectrum in the topological phase. For all parameters, the system is in an MBL phase characterized by a Poissonian tail (the fit interval has been limited to $r > 0.4$ for $\sigma_V = 0.1$ and $r > 0.25$ for $\sigma_V = 0.5, 1.0$ to exclude the peak at $r = 0$). *Bottom panel:* Relative weight of the Poissonian tail for fixed $\sigma_h = 0.05$ and various L . The number of evaluated disorder realizations is here 99 as well.

Entanglement negativity and bi-partite fluctuations. Next, we turn to discussing the entanglement properties of the system. Concomitant with many-body localization, we expected generic eigenstates to exhibit an *entanglement area (volume) law*³⁰ in a localized (ergodic) phase. In a system with a degenerate spectrum, the standard bi-partite entanglement entropy does not capture entanglement: It intertwines classical and genuine quantum correlations. From the perspective of entanglement theory, the entanglement entropy is a valid *entanglement measure*^{31,32} for pure but not for mixed quantum states. From the perspective of numerical stability, the entanglement entropy is at the same time not a stable quantity in situations

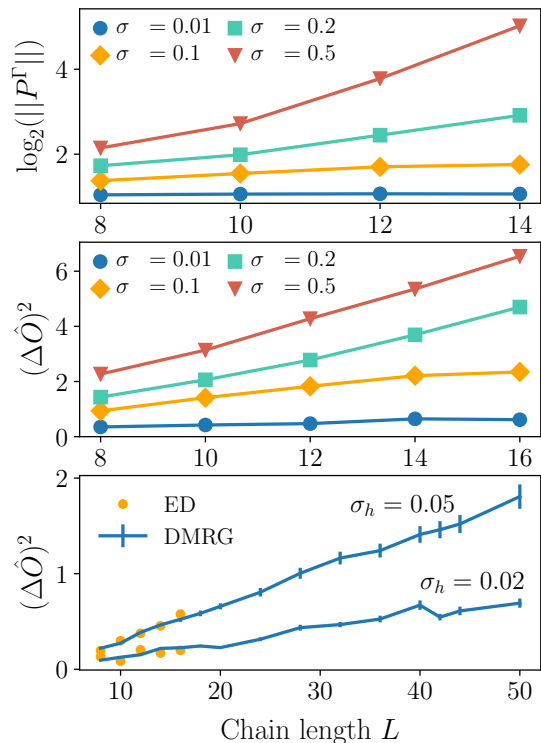


FIG. 3. Scaling of the entanglement negativity (upper panel) and the three-site spin fluctuations (middle panel) with the system size for fixed $\sigma_h = 0.05$ and various σ_V . The localization length becomes larger than $L = 16$ for $\sigma_V \sim 0.15$ (the AGR indicates that the system is localized for any σ_V , see Fig. 2). Bottom Panel: Comparison of DMRG-X and ED data for the three-site spin fluctuations at $\sigma_V = 0$ and for $\sigma_h = 0.02$ as well as $\sigma_h = 0.05$. The DMRG-X curve suggests a slow, possibly logarithmic behavior in the MBL phase. All data evaluated through exact diagonalization shown here represent an average over at least 99 disorder realizations. For the DMRG-X data, at least 440 disorder realizations were carried out with a local bond dimension $\chi = 16$ and the energy variance $\langle \phi | H^2 | \phi \rangle - \langle \phi | H | \phi \rangle^2$ being smaller than 10^{-10} for $\sigma_h = 0.02$ and $5 \cdot 10^{-5}$ for $\sigma_h = 0.05$.

in which degeneracies are smaller than machine precision (see the supplemental material for details). For this reason, we resort to the logarithmic *entanglement negativity*.^{33,34} Both the negativity and its logarithmic counterpart are faithful entanglement measures also for mixed quantum states.³⁵⁻³⁷ It is defined as

$$E_N(\rho) = \log_2 \|\rho^\Gamma\|_1 \quad (2)$$

for a (pure or mixed) density operator ρ , where ρ^Γ denotes the partial transpose of ρ in any basis of a distinguished subsystem. We stress that the use of the entanglement negativity instead of the entanglement entropy is required in any quantum many-body setting in which degeneracies in sub-spaces are becoming exponentially small in the system size.

We complement this analysis by studying the bi-partite fluctuations of $\{O_i\}$ (the analogue of the bi-partite spin fluctuations considered for the XXZ chain). Results are shown in

the top and middle panel of Fig. 3. For small σ_V , we observe an area law. At $\sigma_V \sim 0.1$, both quantities saturate around $L = 14$, and for even larger σ_V , we see volume-law behavior on the accessible system sizes. This implies that the localization length becomes larger than L for these parameters and casts doubts whether or not the transition from the topological to the trivial phase, which we observe for similar parameters (see Fig. 1), is an artifact of small system sizes and that the topological phase in fact remains stable for larger values of σ_h and σ_V (note, however, that the system becomes a trivial insulator in the Ising limit $\sigma_h, \sigma_V \rightarrow \infty$).

DMRG-X. The DMRG-X method allows one to determine the matrix product state representation of a highly-excited, area-law obeying eigenstate in a MBL system even if the energy spacings are smaller than machine precision. It relies on the fact that eigenstates which are close in energy differ substantially in their spatial structure. In our case, the spectrum in the topological phase is (nearly) fourfold degenerate due to the edge excitations, and the corresponding states are almost identical in the bulk. One would thus expect that the DMRG-X cannot reliably resolve the eigenstates that differ only on their edges but instead yields a superposition (within the nearly four-fold degenerate subspaces) that minimizes the entanglement. This is analyzed in detail in the supplemental material.

In contrast, the fluctuations of $\{O_i\}$ (which are dominated by the bulk) can alternatively be calculated via the DMRG-X for much larger system sizes than those accessible via ED. Results are shown in the bottom panel of Fig. 3 and are consistent between DMRG-X and ED for the system sizes accessible to both. Going beyond the ED results in system size one observes a slow growth of the bi-partite $\{O_i\}$ fluctuations, which seems consistent with either logarithmic or linear growth in system size. There are several possible interpretations for this result: (i) The growth of fluctuations is linear and becomes logarithmic or constant only only at larger system sizes than accessible to us; this would however mean that the localization length is very large (although the perturbations are very small) or (ii) the localization length is actually small compared to the system sizes we study and the behavior we see

is truly logarithmic, which is difficult to distinguish on the scales accessible³⁸.

Conclusions. We have characterized the interplay of many-body localization physics and topology in a spin model where these phases can coexist instead of excluding each other using a combination of exact diagonalization and DMRG-X methods. We have explained in what precise sense the entanglement entropy ceases to be a useful quantity to characterize many-body localization in the presence of topological order due to the degeneracy of the spectrum linked to edge excitations and introduced the entanglement negativity as its natural replacement. Using this tool as well as the adjacent gap ratio, we can map out the full phase diagram including the topological-trivial transition with the many-body localized spin system under scrutiny. While the entropy negativity is beyond a DMRG-X ansatz in the topological phase of the diagram (due to a superposition of states which are degenerate and differ locally in space only by edge excitations), other quantities (which are dominated by the bulk) such as bi-partite fluctuations of local operators should still be determined faithfully. Using this we gain access to system sizes far beyond the limitations of exact diagonalization and find a sluggish growth of bi-partite fluctuations of local observables, which is consistent with both linear or logarithmic behavior (which is difficult to distinguish even on these larger system sizes). This leaves two likely conclusions: either the behavior is linear meaning that the localization length is surprisingly large in the system studied or the behavior is logarithmic, which unambiguously can be proven only at even larger system sizes and should be subject of future investigations. It is the hope that the present work — bringing together ideas of condensed matter and quantum information theory — provides a machinery to identify phases of matter and further flesh out the interplay of disorder and topological signatures.

Acknowledgments. This work has been supported by the DFG (CRC 183, FOR 2724, EI 519/14-1, EI 519/15-1) and through the Emmy Noether program (KA 3360/2-1), the ERC (TAQ), and the Templeton Foundation. This work has also received funding from the European Union’s Horizon 2020 research and innovation program under grant agreement No 817482 (PASQuanS).

¹ D. M. Basko, I. L. Aleiner, and B. L. Altshuler, *Ann. Phys.* **321**, 1126 (2006).
² J. Z. Imbrie, “On many-body localization for quantum spin chains,” *ArXiv:1403.7837*.
³ R. Nandkishore and D. A. Huse, *Ann. Rev. Cond. Matt. Phys.* **6**, 15 (2015), *arXiv:1404.0686*.
⁴ J. Eisert, M. Friesdorf, and C. Gogolin, *Nature Phys* **11**, 124 (2015), *arXiv:1408.5148*.
⁵ A. Polkovnikov, K. Sengupta, A. Silva, and M. Vengalattore, *Rev. Mod. Phys.* **83**, 863 (2011).
⁶ C. Gogolin and J. Eisert, *Rep. Prog. Phys.* **79**, 56001 (2016).
⁷ D. A. Huse, R. Nandkishore, and V. Oganesyan, *Phys. Rev. B* **90**, 174202 (2014).
⁸ B. Bauer and C. Nayak, *J. Stat. Mech.* **P09005** (2013).
⁹ M. Friesdorf, A. H. Werner, W. Brown, V. B. Scholz, and J. Eisert,

Phys. Rev. Lett. **114** (2015).
¹⁰ M. Znidaric, T. Prosen, and P. Prelovsek, *Phys. Rev. B* **77**, 064426 (2008).
¹¹ J. H. Bardarson, F. Pollmann, and J. E. Moore, *Phys. Rev. Lett.* **109**, 017202 (2012).
¹² A. Pal and D. A. Huse, *Phys. Rev. B* **82**, 174411 (2010).
¹³ J. A. Kjäll, J. H. Bardarson, and F. Pollmann, *Phys. Rev. Lett.* **113**, 107204 (2014).
¹⁴ R. Vosk, D. A. Huse, and E. Altman, *Phys. Rev. X* **5**, 031032 (2015).
¹⁵ D. J. Luitz, N. Laflorencie, and F. Alet, *Phys. Rev. B* **91**, 081103 (2015).
¹⁶ A. C. Potter, R. Vasseur, and S. A. Parameswaran, *Phys. Rev. X* **5**, 031033 (2015).
¹⁷ D. A. Huse, R. Nandkishore, V. Oganesyan, A. Pal, and S. L.

- Sondhi, Phys. Rev. B **88**, 014206 (2013).
- ¹⁸ A. Chandran, V. Khemani, C. R. Laumann, and S. L. Sondhi, Phys. Rev. B **89**, 144201 (2014).
- ¹⁹ Y. Bahri, R. Vosk, E. Altman, and A. Vishwanath, Nat. Comm. **6**, 7341 (2015).
- ²⁰ R. Orús, Ann. Phys. **349**, 117 (2014).
- ²¹ F. Verstraete, J. I. Cirac, and V. Murg, Adv. Phys. **57**, 143 (2008).
- ²² J. Eisert, Mod. Sim. **3**, 520 (2013).
- ²³ D. M. Kennes and C. Karrasch, Phys. Rev. B **93**, 245129 (2016).
- ²⁴ S. P. Lim and D. N. Sheng, Phys. Rev. B **94**, 045111 (2016).
- ²⁵ X. Yu, D. Pekker, and B. K. Clark, Phys. Rev. Lett. **118**, 017201 (2017).
- ²⁶ V. Khemani, F. Pollmann, and S. L. Sondhi, Phys. Rev. Lett. **116**, 247204 (2016).
- ²⁷ S. R. White, Phys. Rev. Lett. **69**, 2863 (1992).
- ²⁸ N. Y. Yao, C. R. Laumann, and A. Vishwanath, ArXiv e-prints (2015), arXiv:1508.06995 [quant-ph].
- ²⁹ M. Goihl, C. Krumnow, M. Gluza, J. Eisert, and N. Tarantino, ArXiv:1901.02891.
- ³⁰ J. Eisert, M. Cramer, and M. B. Plenio, Rev. Mod. Phys. **82**, 277 (2010).
- ³¹ R. Horodecki, P. Horodecki, M. Horodecki, and K. Horodecki, Rev. Mod. Phys. **81**, 865 (2009).
- ³² M. B. Plenio and S. Virmani, Quant. Inf. Comp. **7**, 1 (2007).
- ³³ K. Zyczkowski, P. Horodecki, A. Sanpera, and M. Lewenstein, Phys. Rev. A **58**, 883 (1998).
- ³⁴ J. Eisert and M. B. Plenio, J. Mod. Opt. **46**, 145 (1999).
- ³⁵ J. Eisert, “Entanglement in quantum information theory,” (2001), PhD thesis, University of Potsdam.
- ³⁶ G. Vidal and R. F. Werner, Phys. Rev. A **65**, 032314 (2002).
- ³⁷ M. B. Plenio, Phys. Rev. Lett. **95**, 090503 (2005).
- ³⁸ In principle a third option would be that the DMRG-X method abruptly becomes unreliable at $L > 16$ while it is perfectly in line with the ED $L \leq 16$ data. Since the agreement up to the largest system sizes accessible with ED is very convincing and there is no abrupt change in the behavior of the DMRG-X results, it is reasonable to assume that this interpretation is unlikely.

SUPPLEMENTAL MATERIAL

DMRG-X as a tensor network method

The DMRG-X method is a tensor network method that has been introduced in Ref.¹ as a tool to determine the matrix product state representation of a highly-excited but localized eigenstate in a disordered system in one spatial dimension. The fact that eigenstates generically satisfy area laws for entanglement entropies in the many-body localized regime^{2,3} renders the method applicable. The method was been developed and tested for the disordered XXZ chain governed by $H = \sum_i (\sigma_i^x \sigma_{i+1}^x + \sigma_i^y \sigma_{i+1}^y + \sigma_i^z \sigma_{i+1}^z + h_i \sigma_i^z)$, where h_i are random fields for each i . The key idea is to prepare the system in a random product state in z direction, which becomes an eigenstate of H in the limit of large h_i . Thereafter, DMRG sweeps are carried out, but instead of choosing the lowest-energy state during each 1 or 2-site DMRG step (as is done for a ground state calculation), one picks the state which has maximum overlap with the prior state. This accounts for the fact that localized eigenstates which have similar energy differ vastly in their spatial structure, and one can determine the matrix product state representation of an excited eigenstate with up to machine precision.

This DMRG-X method can be generalized straightforwardly to the Hamiltonian at hand. One prepares the system in an eigenstate of H_0 , each of which can be written as a matrix product state with a bond dimension of $\chi = 2$ (see the main text). In practice, these states can be constructed using a simple recursive algorithm.

In Fig. S1, we show the energy variance as well as the truncation error as a function of the DMRG-X sweeps for a system with $\sigma_h = 0.05$, $\sigma_V = 0$, and $L = 50$. The bond dimension χ

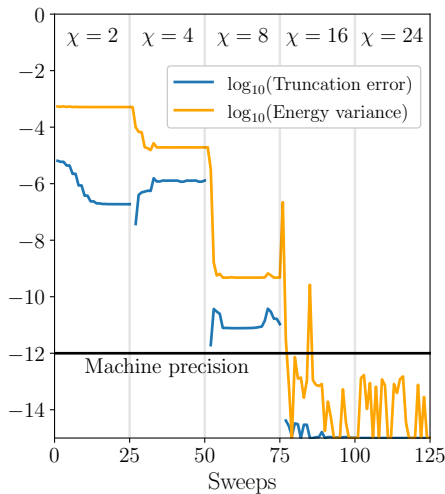


FIG. S1. Evolution of the truncation error and energy variance during the DMRG-X sweeps for $\sigma_h = 0.05$, $\sigma_V = 0$, $L = 50$. The system is initially prepared in a mid-spectrum state of H_0 . The bond dimension χ is successively increased. When we double χ , the truncation error is zero during the next sweep explaining why the logarithm of the truncation error is missing at the points where χ is doubled.

is successively increased, and one eventually obtains an eigenstate of the system up to machine precision. The data shown in the bottom panel of Fig. 3 was obtained this way (although not to $\chi = 24$); the DMRG-X and the ED results agree within the error bar (which stems from the disorder sampling). However, this result needs to be taken with caution, as we will now discuss.

Entanglement entropy for nearly-degenerate spectra and the failure of DMRG-X

In Fig. S2, we show the naively-computed bi-partite entanglement entropy for the same parameters as used in the bottom panel of Fig. 3. One can see that for $L = 8, 10$, the results agree with those obtained via ED. For larger L , the DMRG-X data is smaller than the ED result. This is counter-intuitive (due to the expected area law) and can be understood as follows. The spectrum of H is four-fold degenerate up to finite-size corrections. Any numerical method is bound by machine precision, and one would expect that as L is increased, the DMRG-X can no longer discern between two almost-degenerate states and will converge into a superposition of states which minimizes the entanglement. This is a consequence of a bias towards low entanglement states in the DMRG and DMRG-X, respectively.

In order to confirm this scenario, we determine an eigenstate for $L = 14$ using the DMRG-X (for the parameters of Fig. S2 where the DMRG-X yields an entanglement entropy which is smaller than the ED result). We then calculate the entire spectrum via ED and compute the overlap of the DMRG-X state with all eigenstates. We find that the DMRG-X state is in fact a superposition of *two* states which are close in energy (but whose energy difference can still be resolved within the ED). The superposition of these states has a smaller entanglement than each individual state (see Fig. S3).

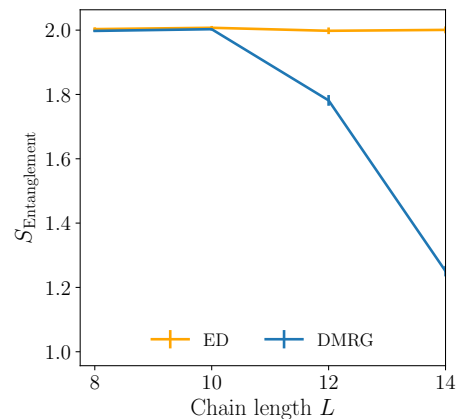


FIG. S2. Bi-partite entanglement entropy as a function of the system size for $\sigma_h = 0.05$, $\sigma_V = 0$. The DMRG-X result deviates from the ED prediction for $L \geq 12$. This is due to the four-fold degeneracy of the spectrum (up to finite-size corrections) in the topological phase and can be understood in detail from the analysis shown in Fig. S3.

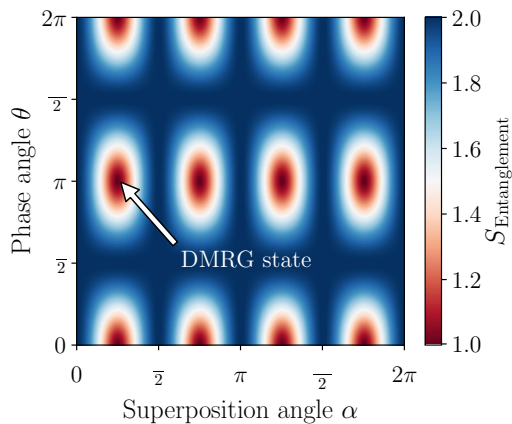


FIG. S3. A single mid-spectrum eigenvector $|\Psi_{\text{DMRG-X}}\rangle$ is determined using the DMRG-X for $\sigma_h = 0.05$, $\sigma_V = 0$, $L = 14$. Thereafter, the Hamiltonian is diagonalized exactly, and the overlap of $|\Psi_{\text{DMRG-X}}\rangle$ with all Hamiltonian eigenvectors is computed. We find that the DMRG-X state is a superposition of two states which are close in energy (but whose degeneracy can still be resolved within the ED), $|\Psi_{\text{DMRG-X}}\rangle = \cos(\alpha)|\Psi_1\rangle + e^{i\phi}\sin(\alpha)|\Psi_2\rangle$. This superposition has a smaller entanglement than $|\Psi_{1,2}\rangle$.

To summarize, in a system with a nearly-degenerate spectrum (such as the one at hand where the edges of an open sys-

tem lead to a four-fold degeneracy), the DMRG-X converges into a superposition of two (or four) eigenstates with minimal entanglement once the error that builds up during all DMRG operations due to machine precision is not sufficient to distinguish these states. One should note that an ED calculation will eventually face the same issue. The fact that the bi-partite spin fluctuations shown in the bottom panel of Fig. 3 agree reasonably with ED can be interpreted as a sort of ‘local thermalization’ between the (two or four) almost-degenerate eigenstates. However, this remains a hypothesis, and the DMRG-X results in Fig. 3 need to be taken with caution.

Hamiltonians with exact matrix product eigenstates

The above Hamiltonian is an example of a class of Hamiltonians that feature exact matrix product eigenstates by construction. If \tilde{H}_0 is a 1-local Hamiltonian with product eigenstates and h a k -local Hamiltonian consisting of mutually commuting terms, then $H_0 = e^{ih}\tilde{H}_0e^{-ih^\dagger}$ is a $2k - 1$ local Hamiltonian. Since the eigenstates are obtained from products under conjugation, each eigenstate is a matrix product state of bond dimension at most $2^{(2k-1)/2}$, and hence strictly localized, satisfying an exact entanglement area law for every Renyi entropy.⁴

¹ V. Khemani, F. Pollmann, and S. L. Sondhi, Phys. Rev. Lett. **116**, 247204 (2016).

² R. Nandkishore and D. A. Huse, Ann. Rev. Cond. Matt. Phys. **6**, 15 (2015), arXiv:1404.0686.

³ B. Bauer and C. Nayak, J. Stat. Mech. **P09005** (2013).

⁴ J. Eisert, M. Cramer, and M. B. Plenio, Rev. Mod. Phys. **82**, 277 (2010).